

CHAPTER 179

Verification of the Consequences of Wavedirectionality on the Loading of Long Coastal Structures by Field Experiments

J. van Heteren *
H.C. Botma **
A.P. Roskam ***
J.A. Battjes ****

Summary

Field measurements were done at the Haringvliet barrier to verify the theory that loading on long structures shows a considerable reduction if wave directionality is taken into account instead of calculating with uniform long crested waves.

Wave loads were measured with a row of pressure meters at the barrier. Directional parameters of the incoming wave field were calculated from the signals of a 3-component acoustic current meter, mounted 7.5 meter in front of the barrier. These calculations were different from those used for an open sea, since the waves near a reflecting structure are formed by two highly correlated wave fields. The agreement between the results of the measurements and theory is good.

1. Introduction

In the Oosterschelde, one of the sea arms in the southern part of the Netherlands, a storm surge barrier is being built with a length of 4,500 m and an entrance aperture of 14,000 m². At the design of this barrier it turned out that the wave loads on the structure are probably influenced by wave directional properties.

To determine these influences a mathematical model has been developed by Battjes, with the incoming main wave direction, the short crestedness, the wave frequency and the length of the structure element as inputs (Battjes, 1982). It appeared that considerable reductions of wave loads can be expected if wave directionality is incorporated. The mathematical model was verified by comparison with empirical data, but the number of useful data available for this purpose was rather limited. Therefore a field campaign was held at a similar barrier in 1982/1983, covering simultaneous measurements of wave pressures at the barrier and the wave directional spectrum of the approaching waves.

- * J. van Heteren, Senior Engineer, Road and Civil Engineering Department, Rijkswaterstaat, The Hague, The Netherlands.
- ** H.C. Botma, Senior Engineer, TNO-Institute of Applied Physics, Delft, The Netherlands.
- *** A.P. Roskam, Project Engineer, Tidal Waters Directorate, Rijkswaterstaat, The Hague, The Netherlands.
- **** J.A. Battjes, Professor, Dpt. of Civil Engineering, Delft University of Technology, Delft, The Netherlands.

To eliminate the influence of the foreland in front of the barrier, the wave directional spectrum had to be measured close by the barrier. As a consequence these measurements were made in a combination of two highly correlated wave fields: the incoming and the reflected wave field. This complicates the derivation of the wave directional parameters from a 3-component orbital velocity measurement considerably.

2. Measurements

The measurements were made at one of the gates of the storm surge barrier in the Haringvliet, a sea arm near the Oosterschelde. This barrier is directed from south-west to north-east and is sheltered by shoals from the North Sea and for south-westerly gales also by one of the islands (fig. 1). The local water depth ranges from 12 m close by the barrier to 4 m at the shoals.



Figure 1. General Topography

Since the depth in the region close to the barrier is relatively large and the bottom is rather flat, the directionality of the wave field close by the barrier is not influenced by refraction. The tidal range in the area is about 1.8 meter. The front of the barrier is not a plane vertical wall, but a smooth cylindrical shaped steel surface.

Pressure was measured at five positions, distributed horizontally along the barrier, covering a width of 14 m.

In front of the barrier a simple steel frame was fixed, carrying 3 pressure gauges A, B and C and the 3-component acoustic current meter V, see figure 2.

In fact the bodies of all four meters were fixed to the central pole of the frame and the pressure intakes and the velocity sensor were fixed to beams, welded to the pole. This ensures that the measurements are taken in parts of the water where the movements are not disturbed too much by the instrument bodies.

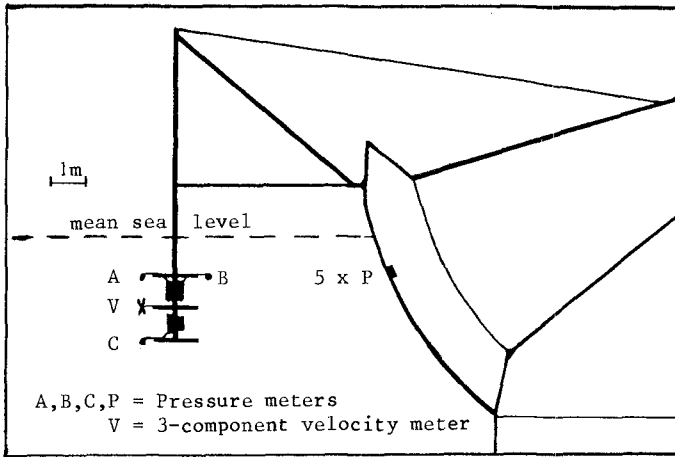


Figure 2. Location of the sensors.

Pressuremeter inlets A and C were positioned in one vertical with 2 m spacing. From pressure signal A the surface waveheights are calculated using linear wave theory. By combining signals A and C linear wave theory could be checked locally. However, afterwards another experiment was performed with simultaneous measurement of surface waves and the associated pressures. The results of these measurements were in good accordance with linear wave theory.

The third pressure gauge B was intended to test standing wave features but it turned out that much more information could be derived from the orbital velocities, so the signals of B were used.

The sensor of the current meter was mounted between pressure intakes A and C. The sensor of this meter is constructed in such a way that it offers little obstruction to the water movements, resulting in good omnidirectional characteristics. It has four pairs of transducers, forming the ends of four measuring lines; the water velocities along these lines are measured using the average traveltime and the travel-time differences for acoustic pulses in both directions. The length of the lines is 23 cm and they are directed parallel to the body diagonals of a cube. Because of the redundancy of using four lines instead of three orthogonal lines, a better omnidirectional uniform sensitivity has been achieved. In case of steady currents one of the lines can be in the wake of one of its own transducers and then it is an advantage not to use that line for the conversion to orthogonal velocities. (In our case the advantage was that the measurements could be continued when one of the four lines became inoperative).

Signals from the 3 pressure gauges A, B, C, the 5 pressure gauges at the barrier and the 4 velocity signals were recorded during 30 minute intervals with a sampling rate of 8 Hertz. Wave height seaward of the shoals was measured too, as well as the wind speed and direction.

During the measuring days, the wind directions ranged from south-west to north-west and speeds from 12 to 19 m/s. The significant wave height seaward of the shoals varied between 0.5 and 3 meters.

3. Calculations

The overall scheme of calculations is given in figure 3.

OBSERVATION	u, v, w	OBSERVATION	$P_1 \dots P_5$
PREPROCESSING		PREPROCESSING	
CROSS SPECTRA	u, v, w	WEIGHTED SUM	P_i
MODEL FITTING	$: \theta_{0,s}$	CROSS SPECTRA	P_1, P_i
LOAD FORMULA	$: G_{\text{theor}}$	LOAD REDUCTION	G_{meas}

Figure 3. The overall calculation scheme

With one procedure the wavefield parameters are estimated and used as inputs to the theory of Battjes to find the wave loading reduction.

With the other procedure the actual wave loading reduction is derived from the pressures at the barrier. Finally the results are compared.

Cross spectral calculations with the three orbital velocity components are the basis of a method for estimating the wave directional parameters. However, the usual method can not be applied in this case, since it is based on the random phase statistical wave theory which does not hold for correlated wave fields. Therefore, the following method has been used. We assume an incoming unimodal directional wave field which is reflected by the barrier. The directional wave energy distribution in this hypothetical wave field is the well known $\cos^2\theta$ model, modified by cancelling all directions from behind the barrier.

For a given wave frequency the wave length is calculated with linear wave theory. Next, the wave field is split up into a series of elementary waves coming from directions at discrete intervals of 4 degrees. Per elementary wave the orbital velocities of the incoming and reflected waves are easily defined taking into account a reflection coefficient R and the distance to a vertical reflecting wall X_0 . (See appendix A).

(In fact, the value of X_0 is not simply the distance between the velocity sensor and the barrier, because of the shape of the front of the barrier. In general, the deviation from the vertical at the water-surface is dependant on the mean water level, which implies a variation in the effective value of X_0 . Without going into details, it can be further assumed that longer waves will show a stronger influence of the deeper, more tilted part of the barrier, increasing the effective tilt compared to the tilt at the surface.

An investigation was made what this implies for waves with directions normal to the barrier and it appeared that the wavelengths as derived from the measured standing wave patterns fit quite well to the wavelengths that can be calculated from linear theory. In fact, the waves are not coming from one normal direction, but as a first estimate this is reasonable).

Per elementary wave the auto and cross spectral components of the orbital velocities are calculated and these spectral components are integrated for all discrete directions. A finer discrimination than 4 degrees did not alter results significantly, it may be that for the smaller values of s even larger directional steps would have been acceptable.

Since the absolute wave height is not relevant to the directional energy distribution, the spectral components from the calculations as well as from the measurements were normalized by dividing with the sum of the 3 autocorrelation components.

Altering the main wave direction Θ_0 , the coefficient s , the effective distance X_0 and the reflection coefficient R results in different sets of integrated spectral components. This is used to search for a combination that shows a minimum of the sum of the squared differences between the normalised spectral components of model and measurements. This part of the method is rather similar to that described by Borgman, (1981). In fact, the reflection coefficient R can be estimated also from the phase relation between the vertical velocity-component w and the horizontal component u , perpendicular to the barrier.

As a result we have per frequency a value of Θ_0 , s and X_0 for a best fit between model and measurements. The parameter X_0 is only used to see if it has a reasonable value, taking into account the influence of wavelength and variable tilt of the reflector plane. It can hardly be expected that the fit of the spectral components will be perfect. This can be illustrated if we look at some special features. In the theoretical model several components can be zero:

$$C_{vw} = 0 \text{ in all cases; } C_{uv} = Q_{uw} = 0 \text{ if } R = 1 \text{ and}$$

$$C_{uv} = Q_{uv} = Q_{vw} = 0 \text{ if } \Theta_0 = 0.$$

w = vertical orbital velocity component
 u = horizontal component normal to barrier
 v = horizontal component parallel to barrier
 C_{ij} = co-spectrum of i and j
 Q_{ij} = quad-spectrum of i and j
 $(S_{ii} = \text{auto spectrum of } i)$
 R = reflection coefficient
 Θ_0 = central wave direction in $\cos^2 s$ distribution.

Figure 4 shows an example of spectral calculations for one measuring interval. Figure 4a shows the sum of the autospectra $S_{tt} = S_{uu} + S_{vv} + S_{ww}$ divided by the peak value of S_{tt} , together with the three autospectra divided by S_{tt} .

Discrepancies with the model are found where the wave energy becomes small relative to the velocity noise. E.g. at low frequencies S_{uu} and S_{ww} show about the same value, where S_{uu} should become much smaller than S_{ww} .

In the frequency range of interest S_{vv} is small, indicating a wave direction nearly normal to the barrier, which is confirmed by the fact that Q_{uv} and Q_{vw} are also small; see figure 4b and 4d.

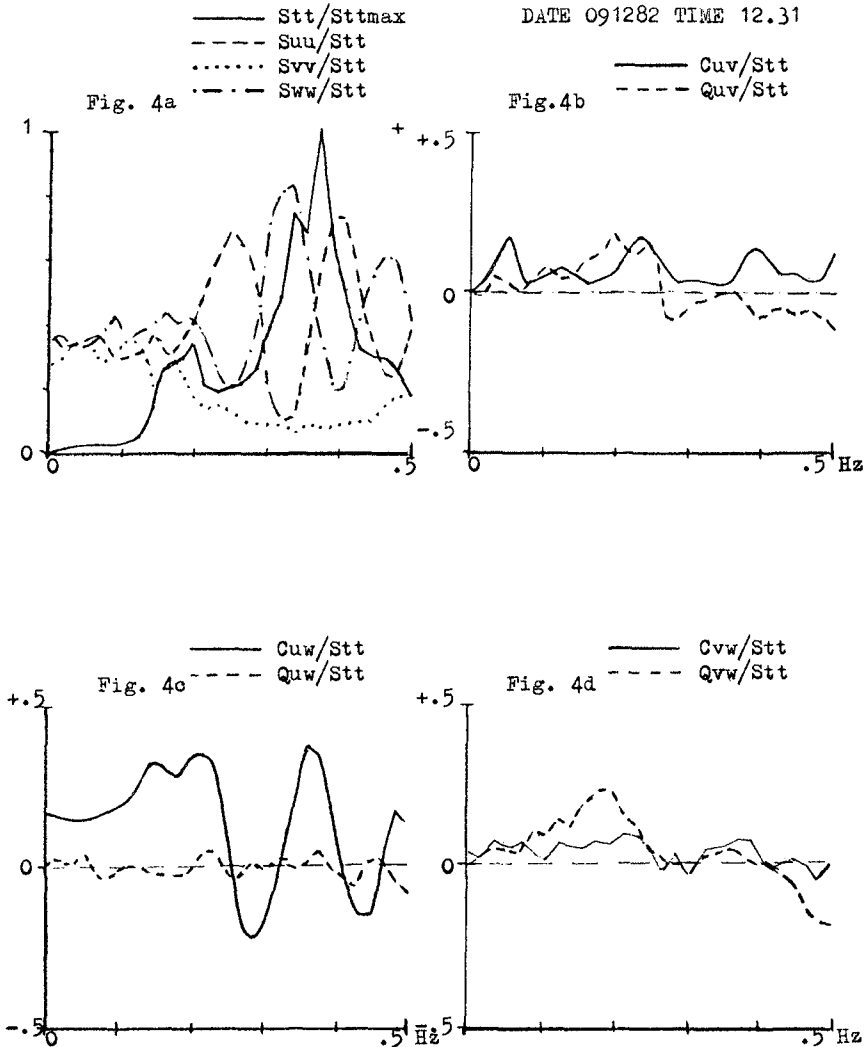


Figure 4. Normalised cross spectra of the orbital velocities.

When comparing the spectra S_{uu} and S_{ww} , the typical standing wave pattern with its nodes and loops can be seen quite distinctly. In general, Q_{uw} is very small; see figure 4c. This means that reflection coefficient R is about 1. Values of R greater than 1 do occur. Physically this means that during the measuring interval the reflected parts of the waves were a bit larger than the incoming parts that swept past the velocity meter. In a short crested wavefield that is quite well possible.

According to the theoretical model C_{vw} should be always zero. The measurements do not show this and this again illustrates that the fit can not be perfect.

Nevertheless the results of this best fit procedure give sufficient confidence to use the central wave direction θ_0 and the spreading parameter s as meaningful values.

A confirmation was found from the fact that the values of θ_0 at high frequencies corresponded to the wind direction. At low frequencies the direction of swell, entering from the North Sea, was found.

With θ_0 and s the wave load reduction can be calculated using the formulae given by Battjes (Ref 1). The results of a typical case are given in figure 5 as G_{theory} .

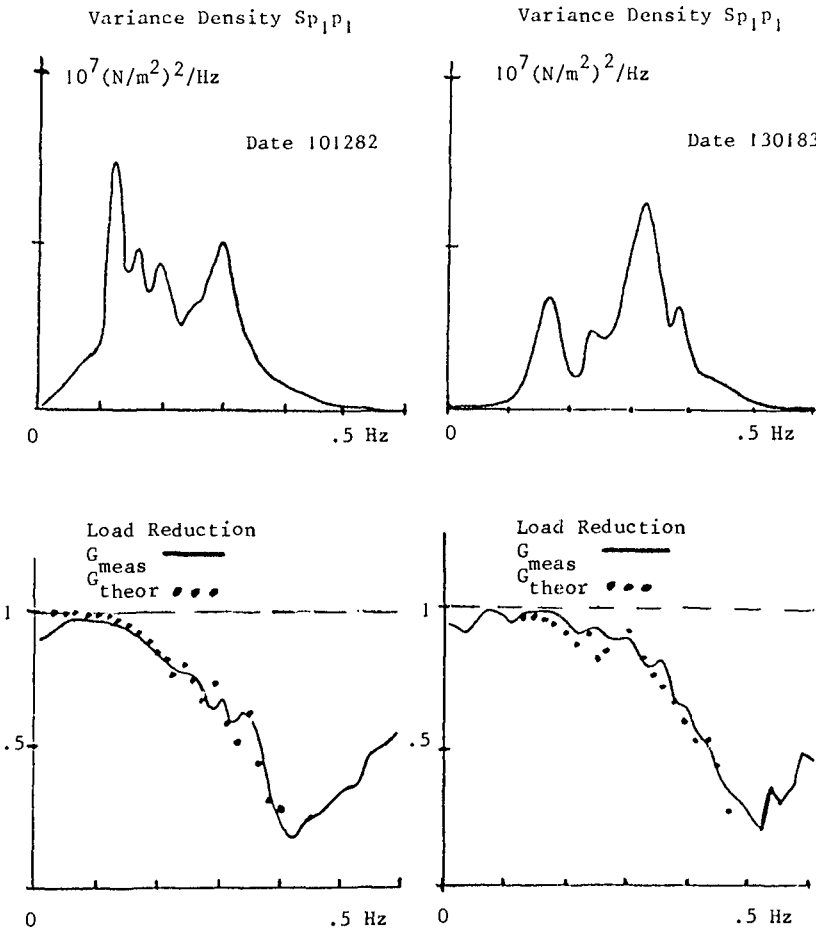


Figure 5. Some results of the waveload verification.

The other calculation path in figure 3 starts with the measured pressure signals at the barrier. After the same preprocessing applied to the other signals, in order to filter out tide and non relevant high frequency noise, the wave load reduction is calculated. The reduction is characterized by the fact that the coherence between pairs of pressure signals decreases if the spacing increases.

By applying to each pressure signal a weight factor, that is representative for a partial area of the barrier, the load reduction can be calculated. The actual load is the sum of products of the partial areas multiplied by the associated pressure signals. The reference load corresponds to the total area multiplied by one of the pressure signals. The results are given in figure 5 as G_{meas} .

Discussion

The agreement between the theoretical and measured load reduction G_{theory} and G_{meas} is very good in the frequency range where the spectral energy is relatively high. At very low frequencies in the formula of Battjes the reduction is 1; the measurement will not reach that value.

Beyond 0.4 Hertz the reduction factor, as calculated from the pressure signals, increases again. This effect is most probably the result of resonant vibrations of the barrier gate and not related to the wave loading.

Conclusions

1. The decrease of the coherence of the wave pressures at the barrier with increasing distance qualitatively indicates that the total load will be lower than the product of one local pressure and the total barrier surface.
2. The quantitative verification shows that the wave load reduction as calculated by Battjes, taking into account the effect of short crestedness, does agree with full scale measurements.
3. In spite of the strong interaction between the incoming and reflected waves due to the short distance to the barrier, the main direction and spreading of the incoming wavefield can be estimated well from the three orthogonal velocity components. The method for this is the fitting of the spectral components from the measurements to the corresponding spectral components of a theoretical wave field that is a combination of the incoming and the reflected waves.

References

- BATTJES, J.A. (1982). Effects of short-crestedness on wave loads on long structures. Applied Ocean Research, 4 (3): 165-172.
- BORGMAN, L.E. (1981). A preliminary examination of the estimation of directional wave spectra, 11 pp. (unpublished report to Rijkswaterstaat)

APPENDIX A

The elementary case of reflection of a long-crested periodic wave is illustrated in fig. A1.

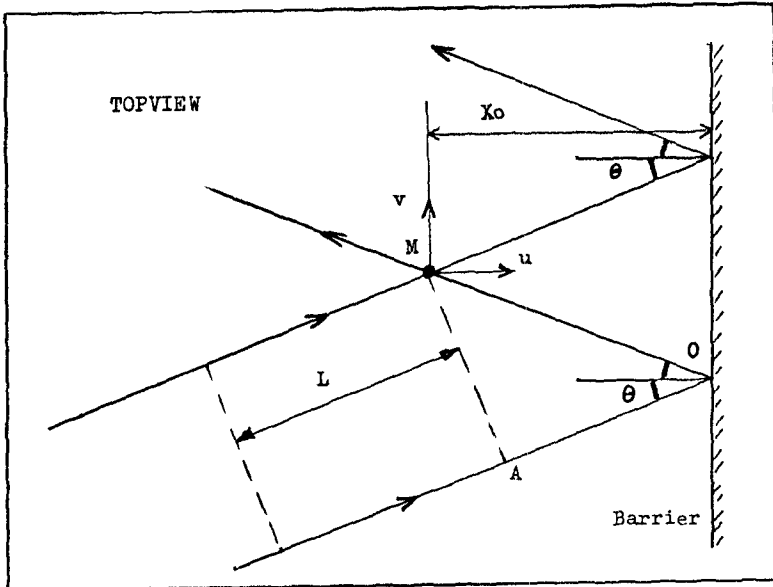


Figure A1. Definition of configuration.

- M measuring point
- X_0 distance from M to the barrier
(The barrier is assumed to be a flat vertical wall)
- L wave length
- Θ incoming wave direction
- u velocity component in direction normal to the barrier
- v velocity component in direction parallel to the barrier
- w vertical velocity component
- R reflection coefficient
- a surface elevation amplitude
- ω frequency
- t time
- H_{uv} ratio between surface elevation and horizontal velocity
- H_w ratio between surface elevation and vertical velocity

In M the distance between the incoming and reflected waves in the direction of propagation is

$$AO + OM = (\cos 2\Theta + 1)OM = (\cos 2\Theta + 1)X_0 / \cos \Theta = 2X_0 \cos \Theta \quad (1)$$

This corresponds to a phase difference

$$\phi = 4 \pi X_0 \cos \Theta / L \quad (2)$$

For the incoming waves in M, we have

$$u = a H_{UV} \cos \theta \sin \omega t \quad (3)$$

$$v = a H_{UV} \sin \theta \sin \omega t \quad (4)$$

$$w = a H_w \cos \omega t \quad (5)$$

At the barrier the wave changes direction in such a way, that the phase of u changes π , while the phase of v and w does not change. We assume that the reflection coefficient R is not associated with a phase shift and that R has the same value for u , v and w . This is a simplification.

So the reflected waves in M are described by

$$u = R a H_{UV} \cos \theta \sin (\omega t - \phi - \pi) \quad (6)$$

$$v = R a H_{UV} \sin \theta \sin (\omega t - \phi) \quad (7)$$

$$w = R a H_w \cos (\omega t - \phi) \quad (8)$$

Adding the incoming and reflected wave signals gives:

$$u = a H_{UV} \cos \theta \left((1-R) \cos \phi / 2 \sin (\omega t - \phi / 2) + (1+R) \sin \phi / 2 \cos (\omega t - \phi / 2) \right) \quad (9)$$

$$v = a H_{UV} \sin \theta \left((1+R) \cos \phi / 2 \sin (\omega t - \phi / 2) + (1-R) \sin \phi / 2 \cos (\omega t - \phi / 2) \right) \quad (10)$$

$$w = a H_w \left(-(1-R) \sin \phi / 2 \sin (\omega t - \phi / 2) + (1+R) \cos \phi / 2 \cos (\omega t - \phi / 2) \right) \quad (11)$$

These velocities give the following spectral components

$$S_{uu} = 0.5 a^2 H_{UV}^2 (1-2R \cos \phi + R^2) \cos^2 \theta \quad (12)$$

$$S_{vv} = 0.5 a^2 H_{UV}^2 (1+2R \cos \phi + R^2) \sin^2 \theta \quad (13)$$

$$S_{ww} = 0.5 a^2 H_w^2 (1+2R \cos \phi + R^2) \quad (14)$$

$$C_{uv} = 0.5 a^2 H_{UV}^2 (1-R^2) \cos \theta \sin \theta \quad (15)$$

$$Q_{uv} = 0.5 a^2 H_{UV}^2 (-2R \sin \phi) \cos \theta \sin \theta \quad (16)$$

$$C_{uw} = 0.5 a^2 H_{UV} H_w (-2R \sin \phi) \cos \theta \quad (17)$$

$$Q_{uw} = 0.5 a^2 H_{UV} H_w (1-R^2) \cos \theta \quad (18)$$

$$C_{vw} = 0 \quad (19)$$

$$Q_{vw} = 0.5 a^2 H_{UV} H_w (1+2R \cos \phi + R^2) \sin \theta \quad (20)$$

In any case $C_{vw} = 0$.

If $R = 0$ the formulae reduce to the normal single wave case.

If $R = 1$ then $C_{uv} = 0$ and $Q_{uw} = 0$ (21)

if $\theta = 0$, then $S_{vv} = 0$, $C_{uv} = 0$, $Q_{uv} = 0$ and $Q_{vw} = 0$ (22)

For each frequency the value of ϕ is calculated via the wavelength L . Then the elementary results (12) to (20) are integrated for various values of θ , at the same time taking a^2 in accordance to a cos-2s directional distribution. For $\theta_0 = 0$ again $C_{uv} = 0$, $Q_{uv} = 0$ and $Q_{uw} = 0$ but S_{vv} is no longer zero, except for infinite s .